European Journal of Pharmaceutical Sciences 206 (2025) 107012

Contents lists available at ScienceDirect

European Journal of Pharmaceutical Sciences

journal homepage: www.elsevier.com/locate/ejps

Heparan sulfate proteoglycan affinity of adeno-associated virus vectors: Implications for retinal gene delivery

Dimitri Romanovsky [1], Hanna Scherk [1], Bastian Föhr, Sabrina Babutzka, Jacqueline Bogedein, Yi Lu, Alice Reschigna, Stylianos Michalakis [*]

Department of Ophthalmology, LMU University Hospital, LMU Munich, Munich, Germany

ARTICLE INFO

Keywords:
Adeno-associated virus
Gene therapy
Virus-receptor interactions
Capsid engineering
Heparin affinity chromatography

ABSTRACT

Adeno-associated virus (AAV)-based vectors have emerged as an effective and widely used technology for somatic gene therapy approaches, including those targeting the retina. A major advantage of the AAV technology is the availability of a large number of serotypes that have either been isolated from nature or produced in the laboratory. These serotypes have different properties in terms of sensitivity to neutralizing antibodies, cellular transduction profile and efficiency. The infectivity of AAV vectors depends on the affinity to certain molecules on the cell surface, in particular to cellular glycosaminoglycans (GAGs) such as heparan sulfate proteoglycans (HSPGs). Here, we tested how altering HSPG affinity in AAV vectors affects cellular tropism and transduction efficiency. The previously developed AAV2.GL variant was used as a starting variant to alter or disrupt HSPG affinity. The HSPG-independent AAV9 serotype was used to introduce different HSPG-binding sites. As an indicator of HSPG affinity, we measured the binding strength of the vector variant on a heparin chromatography column. We show that modification of capsid-exposed residues has a strong impact on HSPG affinity, cellular tropism and transduction efficiency in HeLa cells and in vivo in mouse retina. Our study shows that key properties of AAV vectors can be tailored in different directions and used to improve tropism and efficiency.

1. Introduction

Adeno-associated viruses (AAV) are small non-enveloped viruses that belong to the *Parvoviridae* family. Because of their efficiency in transducing cells, lack of pathogenicity, and favorable immune response profile, they have become promising vectors for gene therapy (Berns and Muzyczka, 2017; Wang et al., 2019). The AAV vectors contain a single-stranded DNA genome that is packaged into a capsid, made of three structural viral proteins (VP1, VP2, VP3) (Xie et al., 2002). The three viral proteins share a common VP3 region but differ in their N-terminal length. The icosahedral capsid is assembled by 5 VP1, 5 VP2 and 50 VP3 proteins. Various AAV serotypes exist (e.g. AAV1, AAV2, AAV9) that differ in the primary sequence of VP1–3 and therefore display varying sensitivity to neutralizing sera (Berns and Muzyczka, 2017; Wang et al., 2019).

A crucial step in AAV infection is the initial binding of the viral capsid to surface molecules of the target cells. The attachment of AAV particles to the cell occurs through the interaction of surface-exposed residues of the capsid with cellular glycosaminoglycans (GAGs), such as heparan sulfate proteoglycans (HSPGs) (Bartlett et al., 2000; Meyer and Chapman, 2022). HSPGs are composed of a protein core with attached heparan sulfate chains. These chains facilitate interaction with various ligands, including the capsid of the most commonly used serotype, AAV2 (Summerford and Samulski, 1998). The key residues for HSPG binding in AAV2 have been identified as amino acids R484, R487, K532, R585 and R588 of VP1 (Kern et al., 2003). These residues are mostly surface-exposed and positively charged, which suggests that electrostatic interactions between positively charged amino acids and negatively charged heparan sulfate may be the key contributor to HSPGbinding of AAV2. Other serotypes such as AAV9 lack the ability to bind HSPG. Instead, the infectivity of AAV9 relies on galactose-containing receptors (Bell et al., 2011; Shen et al., 2011).

Mechanistic knowledge of receptor-capsid interactions is crucial not only for understanding virus behavior, but also for the optimization of viral vectors. Targeted modifications of receptor-binding motifs can enhance transduction efficiency, stability, and tissue specificity (Bennett

* Corresponding author at: Department of Ophthalmology, LMU University Hospital, LMU Munich, Mathildenstr. 8, 80336 Munich, Germany.
E-mail address: michalakis@lmu.de (S. Michalakis).
[1] Shared first authors

https://doi.org/10.1016/j.ejps.2025.107012
Received 8 October 2024; Received in revised form 24 December 2024; Accepted 11 January 2025
Available online 11 January 2025

et al., 2021). In this context, heparin affinity chromatography is an important tool for characterization of receptorbinding of viral vectors. Heparin, a highly sulfated GAG, is structurally very similar to heparan sulfate, and can be used as an affinity resin to purify and characterize AAV particles that bind to HSPG (van Lieshout et al., 2023).

In the present study, we investigated the impact of the HSPG-binding motif RGNR (585–588 in VP1) of AAV2 on transduction efficiency and tropism. For this, we used our previously developed AAV capsid variant AAV2.GL, which contains a 12 amino acid peptide insertion within the HSPG-binding motif (Pavlou et al., 2021). Here, we show that we can alter the HSPG affinity of AAV2.GL by rational design and evaluated how this affects transduction efficiency. Additionally, we artificially introduced an HSPG-binding motif into AAV9 and determined the impact on HSPGbinding and transduction. The presence of the motif correlated with increased HSPG affinity and transduction efficiency. Together our data suggest that modifying, disrupting, or introducing HSPG affinity in AAV vectors can be used to optimize transduction and tailor tropism in cells displaying HSPG.

2. Material and methods

2.1. Cell culture

HEK293T and HeLa cells were maintained in Dulbecco's modified Eagle's medium supplemented with 10 % heat-inactivated fetal calf serum (FCS), 2 mM L-glutamine, and 100 µg each of penicillin and streptomycin/ml at 37 °C in 5 % or 10 % CO_2. Cell counts were performed using the Countess™ II FL and Countess™ cell counting chamber slides (Invitrogen, ThermoFisher Scientific, Germany).

2.2. AAV production and cloning of AAV capsid variants

AAV vectors were produced using a triple plasmid transfection method as previously described (Rieser et al., 2021). All vectors used carried a self-complementary AAV vector genome with a CMV-eGFP (sc.CMV.eGFP) expression cassette as described in (Pavlou et al., 2021). HEK293T cells were cultured in T75 flasks and transfected with AAV vector and helper plasmids using polyethyleneimine (PEI). After 48 h, the cells were removed from the culture dish using a cell scraper and the cell suspension was centrifuged at 4000 x g. Only the pellet was retained for further AAV production according to (Rieser et al., 2021), while the PEI-containing supernatant was discarded to avoid contamination of the chromatographic system. Initial purification was performed via cation exchange chromatography (1mL SO3 column, Sartorius BIA Separation, Slovenia) on an ÄKTA Pure FPLC system, with elution monitored by UV absorbance at 280 nm. The collected fractions were concentrated using Amicon centrifugal filter units with a 100 kDa cutoff to reduce volume and further concentrate AAV particles. This approach effectively separated AAV particles from contaminants, producing high-purity vectors suitable for research applications. Vector genome titers were determined by quantitative PCR (qPCR) as described in (D'Costa et al., 2016). Novel capsid variants have been designed based on previously characterized vector AAV2.GL (Pavlou et al., 2021), and AAV9.WT. Plasmids were produced by either Gibson assembly or site directed mutagenesis of pRC99 (Girod et al., 1999; Nicklin et al., 2001) and prAAV9 (Völkner et al., 2021) plasmids containing the AAV2.GL cap (Pavlou et al., 2021) or AAV9.WT cap, respectively.

2.3. Heparin affinity chromatography

The Heparin Sepharose column (1mL, Sigma, Germany) was equilibrated by washing with 5 column volumes (CV) of binding buffer (100 mM NaCl, pH 7.4) at a flow rate of 1 mL/min using the Patfix system (Sartorius BIA Separations, Slovenia). AAV elution was detected at excitation and emission wavelengths of 280 nm and 350 nm, respectively, using a fluorescence detector (200–650 nm, Satorius, Germany). Vectors were diluted in binding buffer to a concentration of approximately 1×10^{10} viral genomes (vg) per µL. AAV9 variants had to be injected with a titer of 5×10^{9} vg for an equal fluorescence signal. 4 mL of the diluted viral vector solution was loaded onto the equilibrated Heparin Sepharose column at a flow rate of 0.5 mL/min. This step allowed for efficient interaction between the AAV particles and the heparin ligands on the resin. Following sample application, the column was washed with 10 CV of binding buffer at 1 mL/min to remove unbound and loosely bound materials. The column was eluted with increasing NaCl concentrations in the elution buffer, starting from 100 mM NaCl and progressing to 1 M NaCl for 5CV.

2.4. Transduction efficiency assay

HeLa cells were seeded in a 24 well plate (50.000 cells/well) 24 h before the infection. All viral vectors carried a sc.CMV.eGFP expression cassette and were applied in 500 µL and 1000 µL fresh media with a MOI (multiplicity of infections) of 1000 and 10,000 vg/cell (for AAV2 and AAV9 vectors, respectively). The transduction efficiency was calculated as the ratio of the number of eGFP-expressing cells to the number of total cells. Both numbers were counted using the Countess™ II FL and Countess™ cell counting chamber slides (Invitrogen by Thermo Fisher Scientific, Germany).

2.5. Heparin competition assay

HeLa cells were seeded in 24-well plates (50.000 cells/well) 24 h before the infection. AAV2 and AAV9 vectors were pre-incubated with varying concentrations of heparin for 30 min and subsequently applied to the cells at a MOI of 1000 (AAV2) or 10,000 (AAV9). Transduction efficiency was assessed 24 h after infection by quantifying the proportion of eGFP-positive cells using the Countess™ II FL and Countess™ cell counting chamber slides (Invitrogen, ThermoFisher Scientific, Germany).

2.6. Intraocular injections

All animal experiments in this study were conducted in accordance with German laws and were approved by the local authorities (Regierung von Oberbayern). In vivo experiments involving mice were performed under anesthesia induced by a combination of ketamine (100 mg/kg body weight; Medistar GmbH, Germany) and xylazine (10 mg/kg body weight, Xylariem®; Ecuphar GmbH, Germany), diluted in 0.9 % sodium chloride (NaCl 0.9 %, B. Braun, Germany). Anesthesia was administered via intraperitoneal injection.

Adult male and female C57BL6/J mice aged 6 weeks to 3 months were utilized in this study. Pupil dilation was achieved using 0.5 % tropicamide eye drops (Mydriaticum Stulln, Pharma Stulln GmbH, Germany). Injections were performed either freehand or with the UMP3T-1 Microinjection Syringe Pump using the Nanofil Sub-Microliter Injection System (World Precision Instruments, US), equipped with a 34-gauge beveled needle under an Opmi 1 FR pro surgical microscope (Carl Zeiss, Germany).

For intravitreal injections, 1 µL of viral vectors at a dose of 5×10^{9} vg, diluted in PBS-MK (1 mM $MgCl_2$, 2.5 mM KCl, 1 M NaCL in PBS), was carefully injected into the vitreous body of the mouse eye. For subretinal injections, 1 µL of viral vectors at the same dose were administered.

2.7. Immunohistochemical analysis

Following cervical dislocation, mouse eyes were enucleated and fixed in 4 % paraformaldehyde in phosphate buffer (PB) for 1 hour at room temperature. Subsequently, the eyes were incubated overnight in 30 % sucrose in PB and embedded in optimal cutting temperature compound. The primary antibody used was an anti-GFP chicken polyclonal antibody (1:500; GFP-1020, Aves Labs, USA). Cell nuclei in all

sections were stained with DAPI (1:2000; D1306, Thermo Fisher, Germany). Confocal images were acquired using a Leica SP8 confocal laser scanning microscope (Leica Microsystems, Germany), and technical replicates were obtained from different sections. AAV-mediated eGFP transduction was quantified by analyzing the eGFP-positive pixel area in the inner nuclear layer (INL) and outer nuclear layer (ONL) using ImageJ (U. S. National Institutes of Health, Bethesda, USA).

2.8. Statistics

Graphs and statistical analyses were performed using Prism 10 (GraphPad, USA). Results are presented as mean ± SEM. Unpaired Student's *t*-test was used to compare two sample populations. Ordinary one-way ANOVA with Šidák's multiple comparison was used to compare grouped datasets of more than two populations. A significance level of $\alpha = 0.05$ was accepted ($P < 0.05$ *, $P < 0.01$ **, $P < 0.001$ ***, $P < 0.0001$ ****)

3. Results

3.1. Modifications of HSPG affinity in AAV2

HSPG is the primary receptor of AAV2, and its capsid binds HSPG on cellular surfaces as the first step of infection (Summerford and Samulski, 1998). Key for this affinity is the arginine-glycine-asparagine-arginine (RGNR) motif (amino acids 585–588 in VP1), which is located in the loop of VR (variable region) VIII of each of the viral proteins and is found 60 times on the capsid surface (Fig. 1A) (Kern et al., 2003). To investigate the impact of this motif on the tropism and transduction efficiency of the viral vector, we created three AAV2 variants by replacing R588 with a chain of 13 amino acids, thereby disrupting the RGNR motif (Fig. 1B). At the same time, we reintroduced slightly modified versions of this motif in the respective insertions. AAV2.GL retains some HSPG-affinity presumably through a new RAAR motif in which two alanines serve as a spacer between the two arginines (Fig. 1C) (Pavlou et al., 2021). In AAV2.GL.RK, this RAAR motif was altered to RAAK (Fig. 1D). Since lysine (K, $pK_S = 10.28$) has a slightly less positively charged sidechain than arginine (R, $pK_S = 12.1$), we hypothesized that this variant might have a slightly lower affinity for HSPG than AAV2.GL. Lastly, in AAV2.GL.RG, we mutated the RAAR motif to RAAG (Fig. 1E). Glycine (G) is a neutral amino acid without a sidechain. We postulated that this variant exhibits significantly impaired HSPG binding due to disruption of the RAAR HSPG-binding motif.

To test the HSPG affinity of these AAV capsid variants, we performed heparin affinity chromatography, using the heparin resin of the column as a surrogate for HSPG (Xu and Esko, 2014). Wildtype AAV2 (AAV2.WT) exhibited strong binding to the heparin column, with an elution peak at around 40 mS/cm conductivity (Fig. 2A). This result is in line with previous studies (Arnett et al., 2013). AAV2.GL eluted at around 32 mS/cm, whereas AAV2.GL.RK eluted earlier at around 26 mS/cm. Conversely, AAV2.GL.RG did not bind to the column in the application step, suggesting elimination of HSPG affinity when RAAR is changed to RAAG. Overall, these results indicate a weakened interaction between the mutant capsids and heparin and emphasize the strong affinity of the naturally occurring RGNR motif of AAV2.WT for HSPG.

HSPG binding is important for host cell transduction (Summerford and Samulski, 1998). To investigate the effect of the RGNR motif on transduction, we measured the eGFP signal in HeLa cells, after

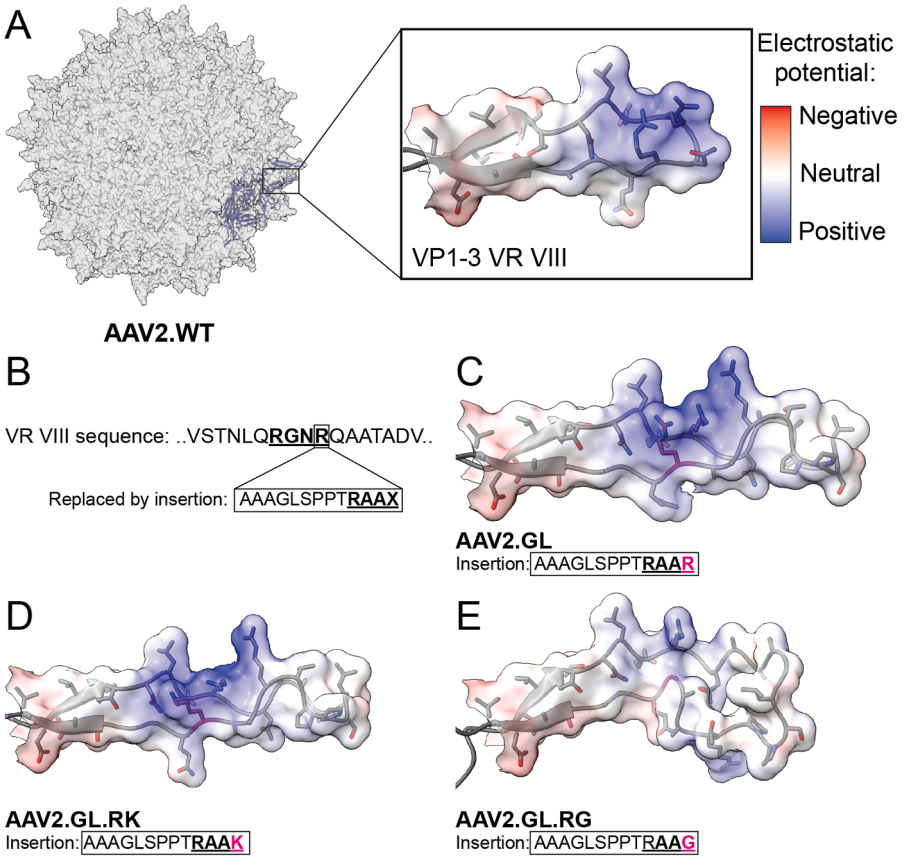

Fig. 1. Overview of AAV2 variants. **A**: Cryo-EM structure of AAV2 zoomed on variable region (VR) VIII (PDB: 8FZ0 by Bennet and McKenna). The surface is colored by coulombic electrostatic potential. **B**: Illustration of the modifications. R588 of AAV2.WT was replaced by the indicated insertion sequence. Underlined sequences represent the (modified) HSPG-binding motif **C-E**: AlphaFold 3 (Abramson et al., 2024) predictions of VR VIII of AAV2.GL (C), AAV2.GL.RK (D) and AAV2.GL.RG (E) variants. Amino acid sequence inserted into wildtype viral protein is indicated. Coloring is the same as in **A**.

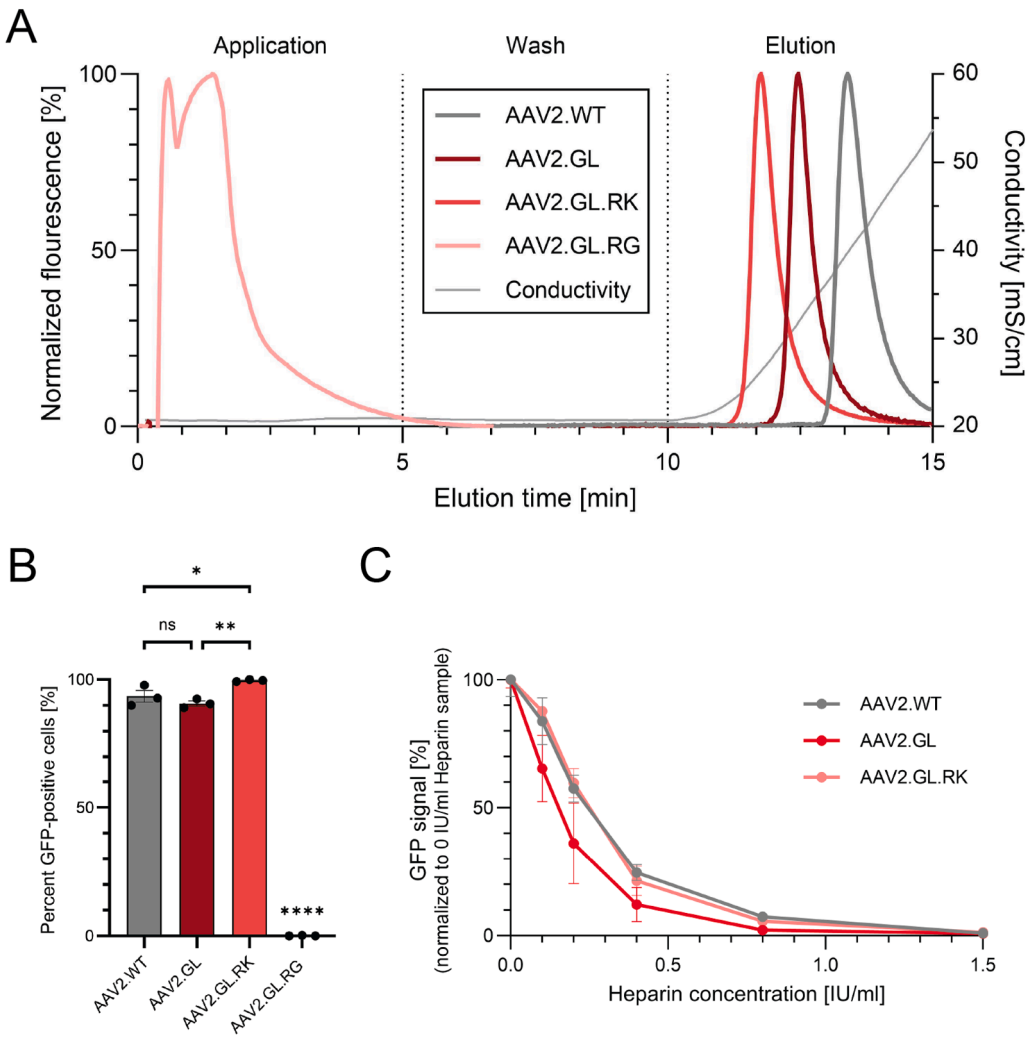

Fig. 2. Evaluation of AAV2 variants in vitro. **A:** Heparin affinity chromatography. AAV2 vector variants were applied onto a heparin affinity resin, washed, and then eluted using a sodium chloride gradient. The fluorescence signal was normalized to the baseline and the maximum value. **B:** In vitro transduction efficiency of AAV2 variants. HeLa cells were transduced with indicated eGFP-expressing AAV2 vectors at an MOI of 1000. Transduction efficiency was determined by counting the percentage of eGFP-positive cells. Biological replicates $n = 3$. Bars show mean ± SEM. One-way ANOVA was used to compare datasets. ($P < 0.05$ *, $P < 0.01$ **, $P < 0.001$ ***, $P < 0.0001$ ****) **C:** HeLa cells were transduced with the indicated eGFP-expressing AAV2 vectors (MOI = 1000 vg/cell) that have been pre-incubated with increasing concentrations of heparin. Heparin-dependent transduction efficiency was determined by normalizing the GFP signal to that of the sample without heparin. Biological replicates $n = 3$. Dots show mean ± SEM.

incubation with viral vectors carrying an eGFP-reporter gene (Fig. 2B). Interestingly, we could detect a significant increase in transduction efficiency of AAV2.GL.RK compared to AAV2.WT and AAV2.GL. However, AAV2.GL.RG completely lost the ability to transduce HeLa cells under these conditions. To further analyze the effect of heparin affinity on transduction efficiency, we performed a heparin competition experiment in which eGFP-expressing AAV2.WT, AAV2.GL and AAV2.GL.RK vectors were incubated with different concentrations of soluble heparin before being applied to HeLa cells. Since AAV2.GL.RG is not able to transduce HeLa cells (Fig. 2B), this variant could not be tested together with the other vectors. We normalized the GFP-signal to that of the sample without soluble heparin, to obtain the heparin-dependent transduction efficiency. With increasing concentrations of heparin, the transduction efficiencies of AAV2.WT, AAV2.GL and AAV2.GL.RK decreased (Fig. 2C). In the presence of 0.8 IU/ml heparin, all three vectors showed a decrease of transduction efficiency of >90 % (Fig. 2C). AAV2.GL transduction was significantly more affected by heparin with an IC50 of 0.140 ± 0.01 IU/ml compared to both, AAV2.WT (0.229 ± 0.005 IU/ml, adjusted p-value: 0.0009, one-way ANOVA) and AAV2.GL.RK (0,235 ± 0,008 IU/ml, adjusted p-value: 0.8768, one-way ANOVA). Whereas AAV2.WT and AAV2.GL.RK transduction in the presence of heparin did not differ significantly from each other (adjusted p-value: 0, 0006, one-way ANOVA).

The interaction between the viral capsid and cellular receptors determines the tropism, i.e. which cell types a virus can transduce. To test if the RAAR HSPG-binding motif is important for viral tropism, we injected AAV2.GL and AAV2.GL.RG into the eyes of wildtype mice. Injections were done either by subretinal or by intravitreal injection, two common ways of administrating ophthalmic drugs and gene therapies (Fig. 3A). After three weeks, the mice were euthanized, and the retina was processed for immunohistochemistry. Cross-sections of the retina were examined under a confocal microscope and the eGFP signal intensity was quantified. AAV2.GL showed the previously described strong transduction pattern of retinal cells (Pavlou et al., 2021) (Fig. 3B). Subretinal injection resulted in slightly better transduction of the ONL and slightly worse transduction of the INL compared to intravitreal injection (Fig. 3C). Interestingly, we observed a profound difference in the performance of AAV2.GL.RG between the two injection methods. The ratio of intravitreal to subretinal transduction efficiency of AAV2.GL.RG was 0.10 ± 0.052 for ONL and 0.16 ± 0.036 for INL. These results

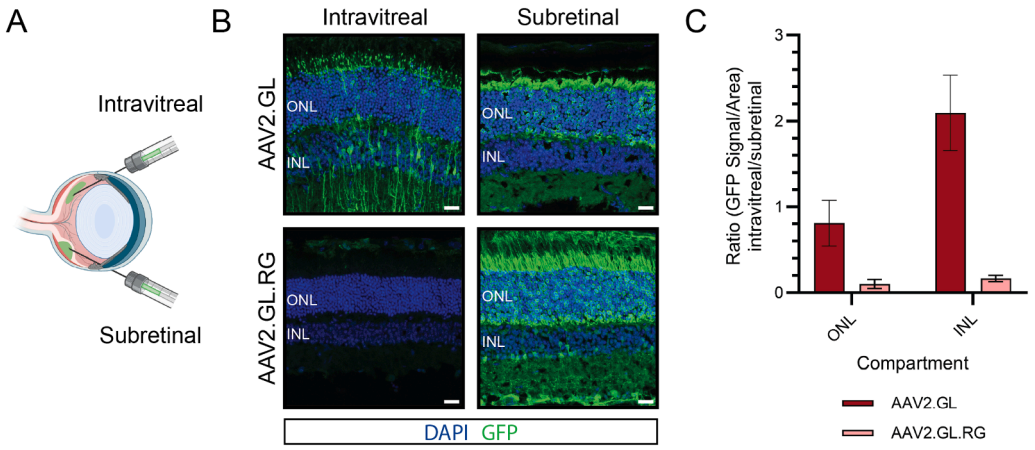

Fig. 3. AAV2 variants perform differently in vivo **A**: Illustration of the subretinal and intravitreal injection method. **B:** In vivo performance of AAV2.GL and AAV2.GL.RG vector variants in the mouse retina. Confocal microscopy images of retinal cross sections three weeks after either intravitreal or subretinal injection of AAV2 variants. Cells were stained with DAPI (blue, nuclei) and immunolabeled for GFP (green, viral reporter). ONL: outer nuclear layer. INL: inner nuclear layer. Scale bar: 20 μm. Biological replicates $n = 3$. **C**: Ratio of AAV vector-mediated eGFP expression after intravitreal and subretinal injection in the inner nuclear layer (INL) and outer nuclear layer (ONL). Biological replicates $n = 3$. Bars show mean ± SEM.

confirm that AAV2.GL.RG is in principle able to transduce retinal cells, but its tropism is highly dependent on the route of administration.

3.2. Introduction of HSPG affinity into HSPG-inert AAV9

In contrast to AAV2, AAV9 possesses no natural affinity for HSPG. Here, we replaced A589 (VP1 of the wildtype AAV9) with the 4 amino acid long RAAR HSPG-binding motif of AAV2.GL (Fig. 4A-B). The aim was to test if we could introduce an HSPG affinity into AAV9 and how that would impact the transduction efficiency. For this, we created two AAV9 variants: AAV9.RAAR contains the RAAR motif (Fig. 4C) whereas AAV9.RAAK contains the slightly less basic RAAK motif (Fig. 4D). Notably, both variants, particularly AAV9.RAAR, exhibited lower production yields than the wild type, which limited our ability to perform biological assays.

Nevertheless, we were able to test the heparin affinity using heparin chromatography. Wildtype AAV9 (AAV9.WT) did not bind to the column and eluted during the application phase (Fig. 4E). While both AAV9.RAAR and AAV9.RAAK also eluted during application, they partially bound to the column and eluted at around 20 mS/cm. Hence, both variants exhibited heparin binding while the wild type does not.

To evaluate the impact of the introduced motif on transduction efficiency, we transduced HeLa cells with AAV9.WT and AAV9.RAAK. Other than the AAV2 variants, these variants required an MOI of 10,000 for efficient transduction of HeLa cells. The low titer of AAV9.RAAR did not allow testing transduction in HeLa cells. Interestingly, we observed a significant increase in transduction efficiency of AAV9.RAAK compared to the wild type (Fig. 4F). This is in line with the observation that the strong HSPG binder AAV2.WT very efficiently transduces HeLa cells at a lower MOI of 1000 (see Fig. 2B). If this increased transduction efficiency of AAV9.RAAK indeed results from the ability to bind HSPG, soluble heparin should act as a competitive inhibitor of transduction (Summerford and Samulski, 1998). To test this, we performed a heparin competition transduction assay. Here, we measured the transduction efficiency of AAV9.WT and AAV9.RAAK in the presence of increasing concentrations of soluble heparin. While the transduction efficiency of AAV9.WT was hardly impacted by soluble heparin, the AAV9.RAAK variant showed a clear dose-dependent decrease in transduction (Fig. 4G). Notably, this effect did not merely compensate for the increase of transduction efficiency of AAV9.RAAK measured in Fig. 4F. Instead, high concentrations of soluble heparin reduced the transduction of AAV9.RAAK to a level significantly lower than AAV9.WT.

4. Discussion

This study explored different modifications of HSPG-binding motifs in the capsid of AAV vectors. We created variants with an altered motif (AAV2.GL), a slightly less basic motif (AAV2.GL.RK), a disrupted motif (AAV2.GL.RG) and a newly introduced motif (AAV9.RAAK and AAV9.RAAR). We tested the AAV capsid variants for HSPG affinity, transduction efficiency and tropism and found that not only the ability to bind HSPG but also the strength of the affinity greatly impacts the performance of AAV vectors.

Using heparin affinity chromatography, we measured heparin affinity as a proxy for HSPG affinity. Although not identical, heparin and heparan sulfate are structurally very similar and heparin is used as a surrogate for heparan sulfate binding due to its broad availability (Xu and Esko, 2014). We designed the variants rationally according to the principle of increasing degrees of alteration. As a starting point, we used AAV2.GL, which was developed earlier in an iterative screening process of an AAV2-peptide display library aiming for improved retinal transduction (Pavlou et al., 2021). AAV2.GL contains a RAAR motif compared to the RGNR motif of AAV2.WT. Since the two crucial arginines are still present we consider this the first degree of alteration of the AAV2.WT HSPG-binding motif. In AAV2.GL.RK, additionally, the second arginine was replaced by a lysine. Lysine is still a positively charged amino acid. Therefore, this variant poses the second degree of alteration. In AAV2.GL.RG the second arginine was replaced by a glycine, which is not charged. We consider this variant the third degree of alteration. In AAV9, the wildtype that hardly possesses natural affinity for HSPG was used as a starting point. Here, we designed our variant sequences to be increasingly similar to the 4 amino acid HSPG-binding motif of AAV2.GL. AAV9.RAAR contains the RAAR motif that poses a first-degree alteration and AAV9.RAAK contains the RAAK motif which is a second-degree alteration of the AAV2.WT. Interestingly, we observed a correlation between the degree of alteration of the AAV2 HSPG-binding motif and the measured heparin affinity. This validates our rational design approach and provides a foundation for more extensive modifications of AAV vectors.

When testing transduction efficiency, we measured no significant changes between AAV2.WT and AAV2.GL. Interestingly, AAV2.GL.RK transduced cells significantly better than AAV2.WT and AAV2.GL, despite showing a lower affinity for heparin. This is not entirely surprising, since (i) viral cell entry is multifactorial and (ii) the relationship between receptor affinity and transduction efficiency is complex. Reducing receptor affinity has been previously shown to enhance

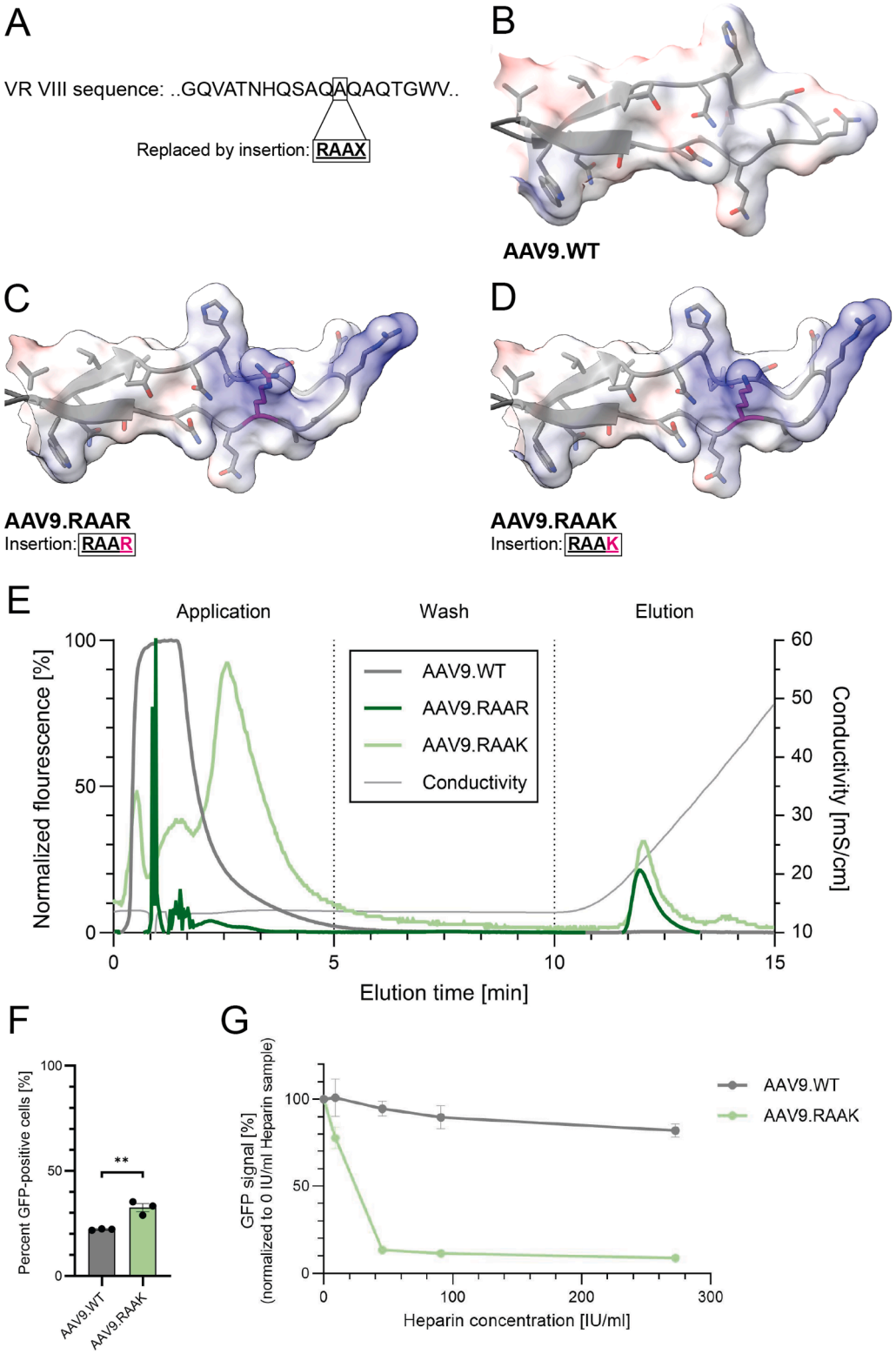

Fig. 4. Introduction of an HSPG-binding motif into AAV9. **A-D:** Overview of the insertions performed. A589 was replaced by a RAAX sequence, where X is either K or R. The loop of AAV9.WT (B) contains no strong positive charge (PDB: 7WJW, (Xu et al., 2022)). Alphafold3 (Abramson et al., 2024) predictions of AAV9.RAAR (C) and AAV9.RAAK (D). Coloring is the same as in Fig. 1A. **E:** Heparin affinity chromatography. AAV9 vector variants were loaded onto a heparin affinity resin, washed, and then eluted using a sodium chloride gradient. **F:** Transduction efficiency of AAV9.WT and AAV9.RAAK. HeLa cells were transduced with AAV9 vector variants carrying a genome with a sc.CMV.eGFP reporter gene expression cassette at a MOI of 10,000. Efficiency of transduction was determined by quantification of the relative number of GFP-positive cells. Bars represent mean ± SEM. Significance determined via unpaired *t*-test (**: $P < 0.01$). **G:** HeLa cells were transduced with the indicated eGFP-expressing AAV9 vectors that have been pre-incubated with increasing concentrations of heparin. Heparin-dependent transduction efficiency was determined by normalizing the GFP signal to that of the sample without heparin.

transduction efficiency in liver (Cabanes-Creus et al., 2020) and co-infusion of soluble HSPG enhanced transduction in the CNS (Mastakov et al., 2002). However, loss of HSPG affinity in AAV2.GL.RG also resulted in an inability to transduce HeLa cells. This suggests that optimal transduction efficiency requires a fine-tuned receptor affinity.

Soluble heparin inhibits the transduction of certain AAV serotypes in cells by competing with heparan sulfate receptors. This has been used previously to determine whether an AAV variant utilizes heparan sulfate receptors for transduction (Halbert et al., 2001; Schmidt et al., 2008; Summerford and Samulski, 1998). We therefore tested AAV2.WT, AAV2.GL and AAV2.GL.RK in heparin competition experiments. The transduction-deficient variant AAV2.GL.RG could not be evaluated in this test, which relies on transduction. Despite the differences observed in heparin affinity chromatography, all three variants showed >90 % inhibition in the presence of 0.8 IU/ml soluble heparin, confirming that they use heparan sulfate receptors for transduction. Interestingly, the transduction efficiency of the AAV2.GL variant, which has a heparin affinity between AAV2.WT and AAV2.GL.RK, was slightly but significantly more sensitive to heparin (IC50 of 0.140 IU/ml) compared to the other two vectors (IC50 of 0.229 and 0.235 IU/ml, respectively). AAV2.WT and AAV2.GL.RK, which showed a stronger divergence on the heparin affinity column, did not differ in the heparin competition assay. This observation emphasizes that cell transduction by AAV vectors is a complex process that depends on multiple factors and cannot be explained by individual receptor affinities, such as HSPG affinity, alone.

When comparing AAV9.WT and AAV9.RAAK regarding their transduction efficiency, we noticed a significant increase in transduction efficiency for AAV9.RAAK. AAV9.WT uses galactose-containing receptors for infection (Shen et al., 2011), and its galactose-binding domain (residues N470, D271, N272, Y446, W503, corresponding to VP1 numbering) is not located in variable region VIII (Bell et al., 2012). We therefore assume that AAV9.RAAK, which we have endowed with an artificial affinity for HSPG receptors, retains the natural affinity for galactose-containing receptors. It is possible that the increased transduction efficiency is due to the additional affinity to heparan sulfate receptors. To test this, we performed a heparin competition assay and observed a dose-dependent inhibition of transduction efficiency of AAV9.RAAK but not AAV9. This result suggests that AAV9.RAAK uses its gained affinity for HSPG for transduction. Compared to the heparin competition assay performed with the AAV2 vector variants, the outcome of this experiment was in better agreement with the predictions based on the heparin affinity chromatography data. However, the observed inhibition by heparin overcompensated the increase of transduction efficiency observed in the absence of soluble heparin. This is possibly caused by heparin blocking interaction sites for other receptors.

AAV2.GL was developed for improved retinal transduction and holds promise to be used for future gene therapies (Pavlou et al., 2021). Disruption of the RAAR HSPG-binding motif in AAV2.GL.RG completely abolished the ability to transduce HeLa cells. The effect of loss of HSPG affinity on retinal transduction in vivo was highly dependent on the route of administration. Transduction efficiency via subretinal injection was not substantially impacted by disruption of the RAAR HSPG-binding motif. However, when delivered via intravitreal injection AAV2.GL.RG was hardly able to transduce the retina. These results are in line with previous findings obtained with a variant of AAV2 (AAV2-HBKO) in which the two arginines in the RGNR have been mutated to alanines (Sullivan et al., 2018). Like AAV2.GL.RG, AAV2-HBKO vector displayed low-transduction activity following intravitreal delivery to the mouse eye and greater photoreceptor transduction following subretinal delivery.

Our study characterizes the role of HSPG in AAV transduction, which is the primary receptor used by AAV2 (Summerford and Samulski, 1998). The only marketed retinal gene therapy to date, voretigene neparpovec, and several other clinical-stage retinal gene therapy programs use vectors based on the AAV2 capsid or derivatives thereof. In the context of ocular gene therapy, it is of relevance that the retina and adjacent structures are decorated with HSPG (Halfter et al., 2008; Zhang and Johnson, 2021), which affects the distribution of AAV2-based vectors (Boye et al., 2016; Woodard et al., 2016). In particular, the levels of HSPG might change in the diseased eye (Bollineni et al., 1997). Thus, improving our understanding of the role of HSPG in AAV transduction may have clear implications for developing future ocular gene therapies.

Taken together, our data provides additional evidence that rational engineering of the AAV capsid provides a powerful approach to modify, disrupt, or introduce HSPG affinity and thereby customize the tropism and function of AAV vectors. The opportunities to optimize viral vectors are vast and still largely unexplored. As gene therapy becomes more and more established, demand for specific clinical applications will grow. Fine-tuning viral vectors can help in optimizing target cell transduction while simultaneously minimizing off-target effects and immune responses. Therefore, capsid engineering will be an important factor in expanding the range of therapeutic gene therapy applications.

CRediT authorship contribution statement

Dimitri Romanovsky: Writing – review & editing, Writing – original draft, Investigation. **Hanna Scherk:** Writing – review & editing, Investigation. **Bastian Föhr:** Writing – review & editing, Writing – original draft, Visualization. **Sabrina Babutzka:** Investigation. **Jacqueline Bogedein:** Investigation. **Yi Lu:** Investigation. **Alice Reschigna:** Investigation. **Stylianos Michalakis:** Writing – review & editing, Supervision, Project administration, Funding acquisition, Formal analysis, Data curation, Conceptualization.

Declaration of competing interest

S.M. is listed inventor on the related patent application WO/2019/076856 and co-founder of the gene therapy company ViGeneron GmbH. All other authors declare no conflict of interest.

Acknowledgment

This work was supported by a Deutsche Forschungsgemeinschaft (DFG) grant to S.M.. The graphical abstract and the illustration in Fig. 2C were created with Biorender.com software. We thank Johanna Koch and Kerstin Skokann (both LMU) for technical help with vector production and quality control.

Data availability

Data will be made available on request.

References

Abramson, J., Adler, J., Dunger, J., Evans, R., Green, T., Pritzel, A., Ronneberger, O., Willmore, L., Ballard, A.J., Bambrick, J., Bodenstein, S.W., Evans, D.A., Hung, C.-C., O'Neill, M., Reiman, D., Tunyasuvunakool, K., Wu, Z., Žemgulytė, A., Arvaniti, E., Beattie, C., Bertolli, O., Bridgland, A., Cherepanov, A., Congreve, M., Cowen-Rivers, A.I., Cowie, A., Figurnov, M., Fuchs, F.B., Gladman, H., Jain, R., Khan, Y.A., Low, C.M.R., Perlin, K., Potapenko, A., Savy, P., Singh, S., Stecula, A., Thillaisundaram, A., Tong, C., Yakneen, S., Zhong, E.D., Zielinski, M., Žídek, A., Bapst, V., Kohli, P., Jaderberg, M., Hassabis, D., Jumper, J.M., 2024. Accurate structure prediction of biomolecular interactions with AlphaFold 3. Nature 630, 493–500. https://doi.org/10.1038/s41586-024-07487-w.

Arnett, A.L.H., Beutler, L.R., Quintana, A., Allen, J., Finn, E., Palmiter, R.D., Chamberlain, J.S., 2013. Heparin-binding correlates with increased efficiency of AAV1- and AAV6-mediated transduction of striated muscle, but negatively impacts CNS transduction. Gene Ther. 20, 497–503. https://doi.org/10.1038/gt.2012.60.

Bartlett, J.S., Wilcher, R., Samulski, R.J., 2000. Infectious entry pathway of adeno-associated virus and adeno-associated virus vectors. J. Virol. 74, 2777–2785. https://doi.org/10.1128/jvi.74.6.2777-2785.2000.

Bell, C.L., Gurda, B.L., Van Vliet, K., Agbandje-McKenna, M., Wilson, J.M., 2012. Identification of the galactose binding domain of the adeno-associated virus serotype 9 capsid. J. Virol. 86, 7326–7333. https://doi.org/10.1128/JVI.00448-12.

Bell, C.L., Vandenberghe, L.H., Bell, P., Limberis, M.P., Gao, G.-P., Van Vliet, K., Agbandje-McKenna, M., Wilson, J.M., 2011. The AAV9 receptor and its modification

to improve in vivo lung gene transfer in mice. J. Clin. Invest. 121, 2427–2435. https://doi.org/10.1172/JCI57367.

Bennett, A., Hull, J., Jolinon, N., Tordo, J., Moss, K., Binns, E., Mietzsch, M., Hagemann, C., Linden, R.M., Serio, A., Chipman, P., Sousa, D., Broecker, F., Seeberger, P., Henckaerts, E., McKenna, R., Agbandje-McKenna, M., 2021. Comparative structural, biophysical, and receptor binding study of true type and wild type AAV2. J. Struct. Biol. 213, 107795. https://doi.org/10.1016/j.jsb.2021.107795.

Berns, K.I., Muzyczka, N., 2017. AAV: an Overview of Unanswered Questions. Hum. Gene Ther. 28, 308–313. https://doi.org/10.1089/hum.2017.048.

Bollineni, J.S., Alluru, I., Reddi, A.S., 1997. Heparan sulfate proteoglycan synthesis and its expression are decreased in the retina of diabetic rats. Curr. Eye Res. 16, 127–130. https://doi.org/10.1076/ceyr.16.2.127.5089.

Boye, S.L., Bennett, A., Scalabrino, M.L., McCullough, K.T., Van Vliet, K., Choudhury, S., Ruan, Q., Peterson, J., Agbandje-McKenna, M., Boye, S.E., 2016. Impact of Heparan Sulfate Binding on Transduction of Retina by Recombinant Adeno-Associated Virus Vectors. J. Virol. 90, 4215–4231. https://doi.org/10.1128/JVI.00200-16.

Cabanes-Creus, M., Westhaus, A., Navarro, R.G., Baltazar, G., Zhu, E., Amaya, A.K., Liao, S.H.Y., Scott, S., Sallard, E., Dilworth, K.L., Rybicki, A., Drouyer, M., Hallwirth, C.V., Bennett, A., Santilli, G., Thrasher, A.J., Agbandje-McKenna, M., Alexander, I.E., Lisowski, L., 2020. Attenuation of Heparan Sulfate Proteoglycan Binding Enhances In Vivo Transduction of Human Primary Hepatocytes with AAV2. Mol. Ther. Methods Clin. Dev. 17, 1139–1154. https://doi.org/10.1016/j.omtm.2020.05.004.

D'Costa, S., Blouin, V., Broucque, F., Penaud-Budloo, M., François, A., Perez, I.C., Le Bec, C., Moullier, P., Snyder, R.O., Ayuso, E., 2016. Practical utilization of recombinant AAV vector reference standards: focus on vector genomes titration by free ITR qPCR. Mol. Ther. Methods Clin. Dev. 5, 16019. https://doi.org/10.1038/mtm.2016.19.

Girod, A., Ried, M., Wobus, C., Lahm, H., Leike, K., Kleinschmidt, J., Deléage, G., Hallek, M., 1999. Genetic capsid modifications allow efficient re-targeting of adeno-associated virus type 2. Nat. Med. 5, 1052–1056. https://doi.org/10.1038/12491.

Halbert, C.L., Allen, J.M., Miller, A.D., 2001. Adeno-Associated Virus Type 6 (AAV6) Vectors Mediate Efficient Transduction of Airway Epithelial Cells in Mouse Lungs Compared to That of AAV2 Vectors. J. Virol. 75, 6615–6624. https://doi.org/10.1128/jvi.75.14.6615-6624.2001.

Halfter, W., Dong, S., Dong, A., Eller, A.W., Nischt, R., 2008. Origin and turnover of ECM proteins from the inner limiting membrane and vitreous body. Eye (Lond) 22, 1207–1213. https://doi.org/10.1038/eye.2008.19.

Kern, A., Schmidt, K., Leder, C., Müller, O.J., Wobus, C.E., Bettinger, K., Von der Lieth, C. W., King, J.A., Kleinschmidt, J.A., 2003. Identification of a Heparin-Binding Motif on Adeno-Associated Virus Type 2 Capsids. J. Virol. 77, 11072–11081. https://doi.org/10.1128/jvi.77.20.11072-11081.2003.

Mastakov, M.Y., Baer, K., Kotin, R.M., During, M.J., 2002. Recombinant adeno-associated virus serotypes 2- and 5-mediated gene transfer in the mammalian brain: quantitative analysis of heparin co-infusion. Mol. Ther. 5, 371–380. https://doi.org/10.1006/mthe.2002.0564.

Meyer, N.L., Chapman, M.S., 2022. Adeno-associated virus (AAV) cell entry: structural insights. Trends. Microbiol. 30, 432–451. https://doi.org/10.1016/j.tim.2021.09.005.

Nicklin, S.A., Buening, H., Dishart, K.L., de Alwis, M., Girod, A., Hacker, U., Thrasher, A. J., Ali, R.R., Hallek, M., Baker, A.H., 2001. Efficient and selective AAV2-mediated gene transfer directed to human vascular endothelial cells. Mol. Ther. 4, 174–181. https://doi.org/10.1006/mthe.2001.0424.

Pavlou, M., Schön, C., Occelli, L.M., Rossi, A., Meumann, N., Boyd, R.F., Bartoe, J.T., Siedlecki, J., Gerhardt, M.J., Babutzka, S., Bogedein, J., Wagner, J.E., Priglinger, S. G., Biel, M., Petersen-Jones, S.M., Büning, H., Michalakis, S., 2021. Novel AAV capsids for intravitreal gene therapy of photoreceptor disorders. EMBo Mol. Med. 13, e13392. https://doi.org/10.15252/emmm.202013392.

Rieser, R., Koch, J., Faccioli, G., Richter, K., Menzen, T., Biel, M., Winter, G., Michalakis, S., 2021. Comparison of Different Liquid Chromatography-Based Purification Strategies for Adeno-Associated Virus Vectors. Pharmaceutics. 13, 748. https://doi.org/10.3390/pharmaceutics13050748.

Schmidt, M., Voutetakis, A., Afione, S., Zheng, C., Mandikian, D., Chiorini, J.A., 2008. Adeno-Associated Virus Type 12 (AAV12): a Novel AAV Serotype with Sialic Acid- and Heparan Sulfate Proteoglycan-Independent Transduction Activity. J. Virol. 82, 1399–1406. https://doi.org/10.1128/jvi.02012-07.

Shen, S., Bryant, K.D., Brown, S.M., Randell, S.H., Asokan, A., 2011. Terminal N-linked galactose is the primary receptor for adeno-associated virus 9. J. Biol. Chem. 286, 13532–13540. https://doi.org/10.1074/jbc.M110.210922.

Sullivan, J.A., Stanek, L.M., Lukason, M.J., Bu, J., Osmond, S.R., Barry, E.A., O'Riordan, C.R., Shihabuddin, L.S., Cheng, S.H., Scaria, A., 2018. Rationally designed AAV2 and AAVrh8R capsids provide improved transduction in the retina and brain. Gene Ther. 25, 205–219. https://doi.org/10.1038/s41434-018-0017-8.

Summerford, C., Samulski, R.J., 1998. Membrane-associated heparan sulfate proteoglycan is a receptor for adeno-associated virus type 2 virions. J. Virol. 72, 1438–1445. https://doi.org/10.1128/JVI.72.2.1438-1445.1998.

van Lieshout, L.P., Stegelmeier, A.A., Rindler, T.N., Lawder, J.J., Sorensen, D.L., Frost, K. L., Booth, S.A., Bridges, J.P., Wootton, S.K., 2023. Engineered AAV8 capsid acquires heparin and AVB sepharose binding capacity but has altered in vivo transduction efficiency. Gene Ther. 30, 236–244. https://doi.org/10.1038/s41434-020-00198-7.

Völkner, M., Pavlou, M., Büning, H., Michalakis, S., Karl, M.O., 2021. Optimized Adeno-Associated Virus Vectors for Efficient Transduction of Human Retinal Organoids. Hum. Gene Ther. 32, 694–706. https://doi.org/10.1089/hum.2020.321.

Wang, D., Tai, P.W.L., Gao, G., 2019. Adeno-associated virus vector as a platform for gene therapy delivery. Nat. Rev. Drug Discov. 18, 358–378. https://doi.org/10.1038/s41573-019-0012-9.

Woodard, K.T., Liang, K.J., Bennett, W.C., Samulski, R.J., 2016. Heparan Sulfate Binding Promotes Accumulation of Intravitreally Delivered Adeno-associated Viral Vectors at the Retina for Enhanced Transduction but Weakly Influences Tropism. J. Virol. 90, 9878–9888. https://doi.org/10.1128/JVI.01568-16.

Xie, Q., Bu, W., Bhatia, S., Hare, J., Somasundaram, T., Azzi, A., Chapman, M.S., 2002. The atomic structure of adeno-associated virus (AAV-2), a vector for human gene therapy. Proc. Natl. Acad. Sci. u S. a 99, 10405–10410. https://doi.org/10.1073/pnas.162250899.

Xu, D., Esko, J.D., 2014. Demystifying Heparan Sulfate–Protein Interactions. Annu. Rev. Biochem. 83, 129–157. https://doi.org/10.1146/annurev-biochem-060713-035314.

Xu, G., Zhang, R., Li, H., Yin, K., Ma, X., Lou, Z., 2022. Structural basis for the neurotropic AAV9 and the engineered AAVPHP.eB recognition with cellular receptors. Mol. Ther. Methods Clin. Dev. 26, 52–60. https://doi.org/10.1016/j.omtm.2022.05.009.

Zhang, K.Y., Johnson, T.V., 2021. The internal limiting membrane: roles in retinal development and implications for emerging ocular therapies. Exp. Eye Res. 206, 108545. https://doi.org/10.1016/j.exer.2021.108545.